COVER SHEET

Temperature and Strain Measurements with Fiber Optic Sensors for Steel Beams Subjected to Fire

Yi Bao[1], Yizheng Chen[1], Matthew S. Hoehler[2], Christopher M. Smith[2], Matthew Bundy[2], and Genda Chen[1,*]

[1]Department of Civil, Architectural, and Environmental Engineering, Missouri University of Science and Technology, 1870 Miner Circle, Rolla, MO 65409, USA

[2]National Fire Research Laboratory, National Institute of Standards and Technology, 100 Bureau Drive, Stop 8666, Gaithersburg, MD 20899, USA

*Corresponding to Dr. Genda Chen. Email: gchen@mst.edu, Phone: (573)341-4462.

ABSTRACT

This paper presents measurements of high temperatures using a Brillouin scattering based fiber optic sensor and large strains using an extrinsic Fabry-Perot interferometric sensor for assessing the thermo-mechanical behaviors of simply-supported steel beams subjected to combined thermal and mechanical loading. The distributed fiber optic sensor captures detailed, non-uniform temperature distributions that are compared with thermocouple measurements resulting in an average relative difference of less than 5 % at 95 % confidence level. The extrinsic Fabry-Perot interferometric sensor captures large strains at temperatures above 1000 °C. The strain results measured from the distributed fiber optic sensors and extrinsic Fabry-Perot interferometric sensors were compared, and the average relative difference was less than 10 % at 95 % confidence level.

INTRODUCTION

During a fire, the load capacity and stability of steel structures can significantly degrade due to adverse temperature-induced deformations and reduced material properties [1]. To assess the thermo-mechanical conditions of a structure, both temperatures and strains must be known. The current state of practice in experimental fire testing is to measure the temperature and global deformation of specimens and to use analytical models to understand the behavior of the member. Effective tools are lacking to directly measure strains in steel members subjected to fire, reliably and accurately.

Fiber optic sensors have drawn intense research interest in the past decade due to their unique advantages, such as immunity to electromagnetic interference, small size, light weight, and excellent durability and resistance to harsh environments. However, their application to structures in fire has not yet been fully explored. Conventional grating-based fiber optic sensors degrade significantly when heated over 300 °C and typically fail around 600 °C [2], which limits their application in fire. Although their temperature operation range can be increased to 1000 °C through means such as the regenerated fiber Bragg grating technique [2], the grating sensors do not provide spatially distributed measurements, but rather a point

measurement at the grating location. In contrast, fully-distributed fiber optic sensors provide a more detailed picture of the structural thermal field. Based on Brillouin scatterings in optical fiber, Brillouin Optical Time Domain Analysis and Brillouin Optical Time Domain Reflectometry technologies have been developed to measure strain and temperature distributions [3]. However, their spatial resolutions were typically limited to half a meter or larger, which is not precise enough in many applications. Recently, a pulse pre-pump Brillouin Optical Time Domain Analysis (PPP-BODTA) technology was developed with a 2 cm spatial resolution [4].

In this study, distributed fiber optic sensors with PPP-BODTA [5] and extrinsic Fabry-Perot interferometric (EFPI) sensors [6] are employed to measure temperatures and strains in steel beams exposed to fire. The sensors' accuracies and precisions for temperature and strain measurements are compared and evaluated.

WORKING PRINCIPLES

The working principles of the distributed fiber optic sensor and extrinsic Fabry-Perot interferometric sensor are briefly introduced in this section. In this study, all fiber optic sensors were fabricated using telecommunication-grade fused silica single-mode fibers. The fiber cross section consisted of an 8.2 μm glass core and a 125 μm glass cladding [7]. Typically, optical fibers are coated with protective polymer coatings outside of cladding to enhance the mechanical performance [8]. In this study, for strain measurement, the coatings were removed before the fibers were installed on the test specimens. However, for temperature measurement, the coatings could be left and burned off at about 300 °C to 400 °C [9].b

Distributed Fiber Optic Sensor

In this study, PPP-BOTDA based on stimulated Brillouin scatterings in optical fiber was employed. Stimulated Brillouin scatterings result from the interactions between light waves and acoustic waves in optical fiber [2]. PPP-BOTDA measures the Brillouin frequency shift along the optical fiber, which is related to the strain and temperature changes of the optical fiber. For light signals with wavelengths of 1.3 μm to 1.6 μm in single mode fibers, the Brillouin frequency shift is about 9 GHz to 13 GHz. The Brillouin frequency shift increases approximately linearly with increasing tensile strain or temperature when the temperature is not very high (< 400 °C). However, after the optical fiber is exposed to high temperatures, the linear relationships are not satisfied and must be modified [7].

Extrinsic Fabry-Perot Interferometric Sensor

An EFPI sensor typically consists of two parallel reflecting surfaces, which are separated by a cavity, as illustrated in Figure 1. Interference occurs between the multiple reflections of light between the two reflecting surfaces. The reflection spectrum of an EFPI can be described as the wavelength dependent intensity modulation of the input light spectrum [6], which is mainly caused by the optical phase difference between two reflected light beams. Constructive interference occurs if the reflected beams are in phase, and this corresponds to a high-transmission peak. If the reflected beams are out-of-phase, destructive interference

occurs and this corresponds to a reflection minimum. Whether the multiply reflected beams are in phase or not depends on the wavelength (λ) of the incident light (in vacuum), the angle with which the incident light travels through the reflecting surfaces (θ), the physical length of the cavity (L) and the refractive index of the material between the reflecting surfaces (n).

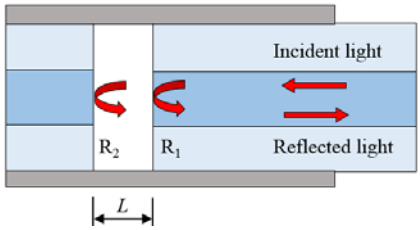

Figure 1. Illustration of a typical EFPI.

The phase difference between each reflected pair of the EFPI is given as:

$$\phi = \frac{2\pi}{\lambda} 2nL\cos(\theta) \tag{1}$$

When perturbation is introduced to the EFPI, the phase difference is influenced with the variation in the optical path length difference of the interferometer. Applying longitudinal strain to the EFPI sensor, for instance, changes the physical length of the cavity, which results in phase variation. By measuring the shift of the wavelength spectrum, the applied strain can be quantified.

EXPERIMENTAL PROGRAM

Test Specimens and Setup

Three S3×5.7 "I-shaped" steel beams were tested with a three-point bending setup in a compartment fire ('flame channel') as shown in Figure 2. Combined temperature and mechanical loading was applied. The three test beams were designated Beam #1, Beam #2, and Beam #3. Each of the beams had a 76 mm depth, 59 mm width, and 1420 mm length. The cross sectional area was 1077 mm^2.

A flame channel, which consisted of a burner rack, an enclosure, and a specimen loading system, was located under a 6 m × 6 m (plan) exhaust hood. The burner rack had four natural gas diffusion burners made of sheet metal, and each of the burners was 300 mm × 300 mm × 140 mm (length × width × height) in dimension. Natural gas entered a burner from the bottom, filled the burner cavity, and then, passed through a ceramic fiber blanket to distribute the gas. The burners were manually regulated by the energy content of the supplied gas, which was measured with an expanded uncertainty of less than 2.4 % [10]. An enclosure constructed of square tube steel, cold-formed steel C-profiles and gypsum board lined with thermal ceramic fiber enclosed the space above the burner rack. The enclosure was open at three faces: the bottom and the two ends in longitudinal direction of the beam, creating the compartment flame dynamics. The heated "compartment" created by the enclosure was approximately 380 mm × 400 mm × 1830 mm (height × width × length) in dimension. Each test beam was simply

supported on two supports constructed of 1-1/2" Schedule 40 pipe, at a 1250 mm clear span. The specimen was loaded by a U-shape 1/2" Schedule 40 pipe (outer diameter: 21 mm) "loading yoke" at the mid-span. The supporting pipes and loading yoke were cooled with the exiting water temperature controlled to less than 50 °C. Load was transferred to the loading yoke with a pulley system.

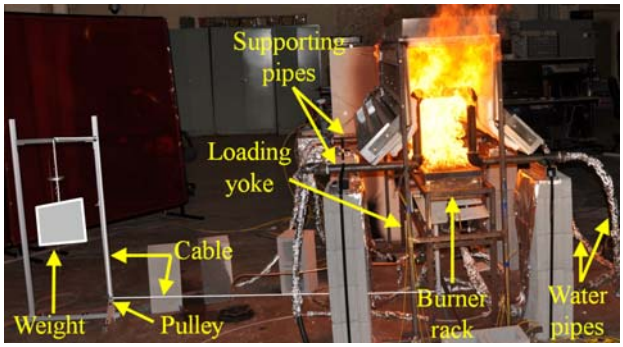

Figure 2. Experimental setup.

Instrumentation of Test Beams

Each beam was instrumented with four glass-sheathed, K-type, bare-bead thermocouples peened into small (diameter < 2 mm) holes, which were drilled into the bottom and top flanges as indicated in Figure 3: TC1 and TC3 at mid-span, and TC2 and TC4 at quarter-span. The thermocouples had a manufacturer-specified temperature standard limit of error of 2.2 °C or 0.75 % (whichever value is greater) over a measurement range of 0 °C to 1250 °C. A calibrated load transducer by Omegadyn was installed on a spanning bar at the bottom of the loading yoke and used to measure the applied load. The linearity and repeatability of the load transducer were ±0.03 % and ±0.01 %, respectively. Each beam was instrumented with one distributed fiber optic sensor (DFO-T) to measure temperature distributions, three distributed fiber optic sensors (DFO-ST1, DFO-ST2, and DFO-ST3) and three EFPI sensors (EFPI1, EFPI2, and EFPI3) to measure strains. The sensors EFPI1, EFPI2, and EFPI3 were closely deployed to DFO-ST1, DFO-ST2, and DFO-ST3, respectively.

Data from the fuel delivery system, thermocouples, displacement sensors and a load transducer were measured continuously using a National Instruments data acquisition system (NI PXIe-1082). Thermocouple data were recorded using 24-bit Thermocouple Input Modules (NI PXIe-4353), and load and displacement data were recorded using a high-speed, 16-bit multifunction module (NI PXIe-6363). Data were sampled at 90 Hz with average values and standard deviations recorded in the output file at a rate of 1 Hz.

A Neubrescope data acquisition system (NBX-7020) for the distributed fiber optic sensors was used to perform PPP-BOTDA measurements with 2 cm spatial resolution and accuracies of 0.75 °C and 15 με for temperature and strain, respectively. In this test, the spatial resolution was 2 cm, meaning that the Brillouin frequency shifts of two points spaced at no less than 2 cm could be distinguished. An optical spectrum analyzer (Yokogawa AQ6370C) was used to acquire data from the extrinsic Fabry-Perot interferometers with a broadband (1470 nm to 1630 nm) light source (Keysight 83437A). The operation wavelength ranged from 1500 nm to 1600 nm. The sampling frequency ranged from 0.2 Hz to 1 Hz.

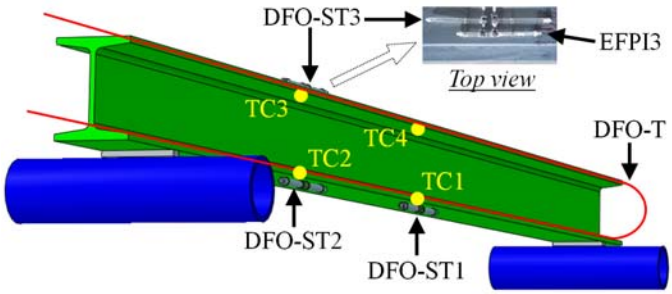

Figure 3. Instrumentation of test beams.

Test Protocol

Each beam was subjected to both fire and mechanical loading. Figure 4 illustrates the fire test protocol.

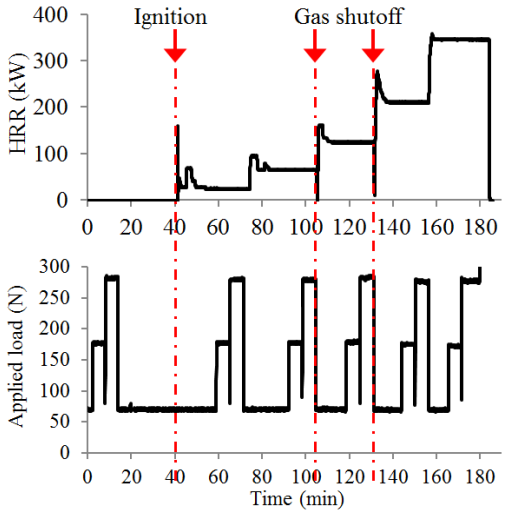

Figure 4. Test protocol.

The heat release rate (HRR) was held approximately constant at five target levels: 25 kW, 65 kW, 120 kW, 195 kW, and 350 kW, which corresponded to beam temperatures at TC1 of approximately 200 °C, 400 °C, 600 °C, 850 °C, and 1050 °C, respectively. During the test of Beam #2, the gas was turned off for about 20 seconds before the HRR was increased to 120 kW and 195 kW, respectively, to allow for visual observation. When the HRR was increased to a higher level, the target value was overshot and then quickly regulated down to the expected value. At each HRR level, in addition to the self-weight, the beam was subjected to three levels of loads at the mid-span. For Beam #1, the three loads were approximately 68 N, 98 N, and 126 N, and sustained for 7 minutes, 4 minutes, and 4 minutes, respectively. For Beams #2 and #3, the three loads were approximately 68 N, 176 N, and 285 N, each sustained for 6 minutes.

EXPERIMENTAL RESULTS AND DISCUSSION

Temperature Measurements

At each sustained HRR level, the beam temperature gradually stabilized to a

temperature with some variation. To quantify the temperature variations, the mean values and standard deviations were calculated over 15 minutes for Beam #1, and 18 minutes for Beams #2 and #3 when the mechanical loads were applied at each temperature level. The coefficient of variation for all the thermocouple readings is less than 4 %. Similarly, to average out the effects of temperature fluctuation, five measurements were made using the DFO-T at each sustained temperature level. Each measurement was an implicit average over a time between 15 seconds and 40 seconds. The DFO-T readings have a maximum coefficient of variation of 4 %, which was similar to that of the thermocouples. The relative difference between the mean temperatures from the DFO-T and the thermocouple ranges from -10 % to 8 %. To understand the statistical significance of the measurement differences, the average of mean temperature differences (four for Beam #1, three for Beam #2, four for Beam #3) was calculated at each HRR level and presented in Figure 5 as an average temperature difference. In addition, the range of mean differences at 95 % confidence level is represented by the error bar.

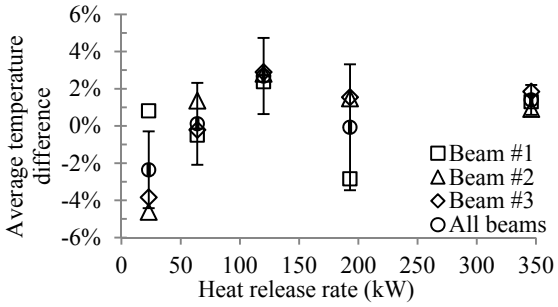

Figure 5. Difference between the fiber optic sensor and thermocouple temperature readings (error bars at 95% confidence).

It can be observed from Figure 5 that the mean difference at 95 % confidence level is less than 5 %, which is acceptable in many engineering applications. The discrepancies may be attributed to several factors. First, the DFO-T sensor was installed in a slightly different location than the thermocouples. Second, the thermocouple beads were located slightly below the surface of the beam and the DFO-T slightly above the surface, and thus, the influence of gas temperature variation on the measurements varied. Additionally, the thermocouples were not corrected for radiation losses.

Strain Measurements

The strain results measured from the EFPI sensors are plotted in Figure 6. As the HRR increases, the strain values approximately linearly increase. When the HRR was no more than 120 kW, the strain results from different sensors attached on different test beams agreed well. At the HRR equal to 120 kW, the strain values were approximately 8000 με to 9000 με. When the HRR became larger than 120 kW, greater variation of the strain results was observed from different sensors deployed at different locations. At the HRR equal to 350 kW, up to 35,300 με (3.53 %) strain was measured by the EFPI sensors.

Similar to the temperature measurements, multiple strain measurements were made from the distributed fiber optic sensors and EFPI sensors at each HRR level. The mean values for the two measurement methods were compared statistically for

the conditions when the HRR was no larger than 120 kW, as shown in Figure 7. The mean strain difference at 95 % confidence level is less than 10 %. There are several reasons for the discrepancy between strain measurements from different sensors. First, the two sensors were deployed at slightly different locations that were subjected to different strains. Second, the data used to calculate the mean values of the two independent sensing systems were not selected at exactly the same moment. Although the two data acquisition systems were synchronized, they had different measurement (reading) durations, and thus, the measurement results were not achieved simultaneously. Third, each instrument has its own accuracy and repeatability at a level, and the measurement results contain error.

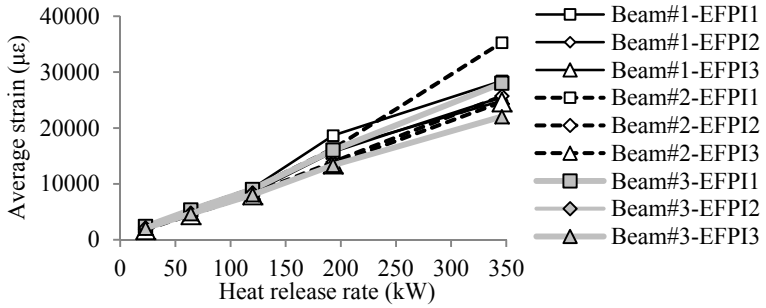

Figure 6. Average strain results measured from EFPI sensors.

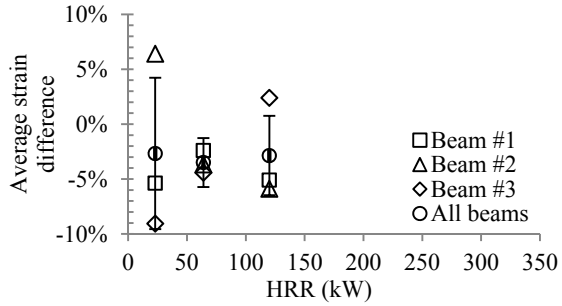

Figure 7. Difference between the distributed fiber optic sensor and EFPI sensor strain readings (error bars at 95% confidence).

CONCLUSIONS

Pulse pre-pump Brillouin Optical Time Domain Analysis distributed fiber optic temperature sensors have been demonstrated at temperatures up to 1050 °C in fire with adequate sensitivity and accuracy for typical structural engineering applications. These measurements add significant value over traditional thermocouples by providing distributed measurements over the length of the optical fiber with a spatial resolution of 2 cm. The measured temperatures were validated by thermocouples resulting in an average relative difference of less than 5 % at 95 % confidence level.

Extrinsic Fabry-Perot interferometric strain sensors have been demonstrated to operate up to 1050 °C in fire and measure at least 35,300 με (3.53 %) strains. The thermal strain predicted from the distributed fiber optic sensor and the extrinsic Farby-Perot interferometric sensor strain results were compared. The mean strain difference at 95 % confidence level was less than 10 %.

These results demonstrate the potential application of fiber optic temperature and strain sensors in structural fire testing. The investigated sensors provide increased temperature resistance, strain capacity, and spatial resolution when compared to traditional methods. Further development of the sensors is required to improve the robustness of the sensors and the speed of installation and measurement.

ACKNOWLEDGEMENT

This work was funded by the National Institute of Standards and Technology (NIST) under Award No. 70NANB13H183. The contents of this paper reflect the views of the authors, and do not necessarily reflect the official views or policies of NIST. Certain commercial equipment, instruments, or materials are identified in this paper to specify the experimental procedure. Such identification is not intended to imply recommendation or endorsement by NIST, nor to imply the materials or equipment are necessarily the best available for the purpose.

REFERENCES

1. Kodur, V., M. Dwaikat, and N. Raut. 2009. “Macroscopic FE model for tracing the fire response of reinforced concrete structures,” Eng. Struct., 31 (10), 2368-2379.
2. Rinaudo, P., B. Torres, I. Paya-Zaforteza, P.A. Calderón, and S. Sales. 2015. “Evaluation of new regenerated fiber Bragg grating high-temperature sensors in an ISO834 fire test,” Fire Safety J., 71, 332-339.
3. Bao, X., and L. Chen. 2011. “Recent progress in Brillouin scattering based fiber sensors.” Sens., 11, 4152-4187.
4. Kishida, K., and C.H. Li. 2006. “Pulse pre-pump-BOTDA technology for new generation of distributed strain measuring system.” Proc. Struct. Health Monit of Intel. Infrastruct., 471-477.
5. Bao, Y., and G. Chen. 2015. “Fully-distributed fiber optic sensor for strain measurement at high temperature.” Proc. 10th Int. Workshop Struct. Health. Monit., Stanford, CA.
6. Rao, Y. J. 2006. “Recent progress in fiber-optic extrinsic Fabry-Perot interferometric sensors,” Opt. Fiber Technol. 12, 227-237.
7. Bao, Y., W. Meng, Y. Chen, G. Chen, K.H. Khayat. 2015. “Measuring mortar shrinkage and cracking by pulse pre-pump Brillouin optical time domain analysis with a single optical fiber,” Mater. Lett. 145, 344-346.
8. Bao Y, G Chen. 2016. “Strain distribution and crack detection in thin unbonded concrete pavement overlays with fully distributed fiber optic sensors.” Opt. Eng. 55(1), 011008.
9. Bao, Y., and G. Chen. 2016. “Temperature-dependent strain and temperature sensitivities of fused silica single mode fiber sensors with pulse pre-pump Brillouin optical time domain analysis,” Mes. Sci. Tech., under review.
10. Bundy, M., A. Hamins, E.L. Johnsson, S.C. Kim, G.H. Ko, and D.B. Lenhert. 2007. “Measurements of heat and combustion products in reduced-scale ventilation-limited compartment fires,” NIST Technical Note 1483.